C. R. Mecanique 341 (2013) 672–686

Contents lists available at ScienceDirect

Comptes Rendus Mecanique

www.sciencedirect.com

The natural frequencies of waves in helical springs

Anis Hamza *, Sami Ayadi, Ezzeddine Hadj-Taïeb

Laboratory of Applied Fluid Mechanics and Modelling, University of Sfax, National Engineering School of Sfax (ENIS), BP 1173, 3038 Sfax, Tunisia

ARTICLE INFO

Article history:
Received 15 January 2013
Accepted 28 September 2013
Available online 23 October 2013

Keywords:
Helical compression springs
Impedance method
Method of Lax–Wendroff
Resonance and beat phenomenon
Poisson coupling

ABSTRACT

In this study, the vibrations of a coil, excited axially, in helical compression springs such as tamping rammers are discussed. The mathematical formulation is comprised of a system of four partial differential equations of first-order hyperbolic type, as the unknown variables are angular and axial deformations and velocities. The numerical resolution is performed by the conservative finite difference scheme of Lax–Wendroff. The impedance method is applied to calculate the frequency spectrum. The results obtained with this method were used to analyze the evolution in time of deformations and velocities in different sections of the spring resulting from a sinusoidal excitation of the axial velocity applied at the end of the spring. These results clearly show the effect of the interaction between the slow axial waves and the fast angular waves, the resonance and other phenomena related to wave propagations such as wave reflections and beat.

1. Introduction

Helical springs are important mechanical components in many industrial applications [1,2]. The springs are elastic elements widespread in all kinds of machinery and equipment. Their functions are very diverse. The main role of the springs is to absorb shock and reduce vibration. Several accidents have been explained by different forms of resonance oscillations of the springs. For this reason, the frequency study must be carefully done.

Love [3] developed the equations to study the static response of helical springs subjected to large deformations. Given their important role, modeling the behavior of the springs was a very interesting objective for a research work in dynamics [4–6]. When a helical spring is subjected to a sudden shock loading, considerable vibration may occur therein [7]. Gironnet and Louradour [8], Yildirim [9] determined the natural frequencies of helical springs.

Resonance is a phenomenon that occurs when the spring is excited by a periodic signal whose frequency is equal to the natural frequency. This phenomenon may be initiated very gradually, and that builds up a steady-oscillatory regime in real situations (unless failure occurs). Moreover, a beating of a transient nature develops when the period of the excitation is not fundamental or harmonic [10]. Various numerical and analytical methods were applied to determine the natural frequencies of resonance of the spring. These include for example: the method of transfer matrix [11], the formulation of the dynamic stiffness [12] and the pseudo spectral method [13].

Yildirim [11] developed a method based on digitalizing the transfer matrix of rigidity to determine the natural frequencies of a helical spring. Becker et al. [14] determined the resonance frequencies of a helical spring subjected to an axial load of static compression. For this, they performed a numerical solution of the linearized equations of motion using the method of transfer matrix. Lee and Thompson [12] developed the equations of motion of helical springs based on the Timoshenko beam theory. The natural frequencies of the spring are obtained by canceling the determinant of the stiffness matrix. Jiang et al. [15] studied the forced vibration and wave propagation in helical springs with reference to partial differential

* Corresponding author.
E-mail address: anis7amza@gmail.com (A. Hamza).

1631-0721/$ – see front matter
http://dx.doi.org/10.1016/j.crme.2013.09.006

equations describing the dynamic behavior of springs subjected to axial force and torque. They based their study on the method of Laplace transform to find an analytical solution in the form of a numeric sequence that describes the vibrations along the spring.

In this paper, we study the numerical propagation of elastic waves in a helical spring following a sinusoidal excitation of the axial velocity. The analytical and numerical models describing wave propagation, in the case of gradual excitations in time, have been prepared by Phillips, Sinha, and Costello [16,17]. The mathematical model is based on those established by Phillips and Costello [16]. The strain evolutions in different sections of the spring due to an excitation of the instantaneous velocity are studied. The impedance method is applied to the mathematical model consisting of four partial differential equations of order one describing the propagation of deformations and velocities along the spring. The mechanical impedance is expressed at any point of the spring and especially at the extremities that represent the most stressed points. The frequency spectra are shown in the impedance diagrams. The numerical solution is carried out by the Lax–Wendroff finite-difference method formulation, based on the conservative linear model. The effect of dynamic coupling, resulting from Poisson's ratio, between axial and angular waves in the spring is studied. The results were used to examine the evolution of angular and axial strains as a function of time at special points of the spring at different vibration frequencies and to show concepts related to the wave propagation phenomena such as resonance and beat.

2. Mathematical formulation

In addition to the usual assumptions of continuum, elastic, homogeneous and isotropic materials, we add the following assumptions: the one-dimensional motion is assumed along the axis of the spring, the terms of friction and volume forces are neglected, the spring coils are not joined and the bending movement is assumed to be zero. The equations of the dynamic behavior of the coil springs are determined by applying a dimensional analysis with reference to the basic formulas of the resistance of materials based on the results given by the general theory of bending and twisting slender rods, established two coupled partial differential equations of second order that represent the equations of wave propagation of the axial and angular movement of the springs [18]. This leads to the following system:

$$\frac{\partial u_t}{\partial t} = a\frac{\partial u_x}{\partial x} + b\frac{\partial v_x}{\partial x} \tag{1}$$

$$\frac{\partial v_t}{\partial t} = b\frac{\partial u_x}{\partial x} + c\frac{\partial v_x}{\partial x} \tag{2}$$

$$\frac{\partial u_x}{\partial t} = \frac{\partial u_t}{\partial x} \tag{3}$$

$$\frac{\partial v_x}{\partial t} = \frac{\partial v_t}{\partial x} \tag{4}$$

where u is the axial displacement of the spring, $v = r\phi$ is the angular displacement, $u_x = \varepsilon = \partial u/\partial x$ is the axial deformation, $u_t = \partial u/\partial t$ is the axial velocity, $v_x = \beta = \partial v/\partial x = r\partial\phi/\partial x$ is the angular deformation and $v_t = \partial v/\partial t = r\partial\phi/\partial t$ is the angular velocity.

This model is a system of four first-order partial differential equations of hyperbolic type. It takes into account all the four unknown u_t, u_x, v_t and v_x that depend on abscissa x and time t, including the dynamic coupling between the axial and angular waves.

In the case of a linear behavior and when the strains are small, i.e. $|u_x| \ll 1$ and $|\upsilon_x| \ll 1$, the coefficients appearing in Eqs. (1) to (4) are defined by:

$$a = \frac{EIh}{Mr^2}\left(1 - \frac{\upsilon}{1+\upsilon}\cos^2\alpha\right)\sin\alpha \tag{5}$$

$$b = -\frac{EIh}{Mr^2}\frac{\upsilon}{1+\upsilon}\sin^2\alpha\cos\alpha \tag{6}$$

$$c = \frac{EIh}{Mr^2}\left(1 - \frac{\upsilon}{1+\upsilon}\sin^2\alpha\right)\sin\alpha \tag{7}$$

Angular deformations and velocities are therefore connected, at any time, to axial deformation and velocities and vice versa. This coupling is due to the effects of Poisson's ratio υ.

3. Numerical solution with the Lax–Wendroff method

The numerical solution of the problem for hyperbolic partial differential equations described by (1), (2), (3) and (4) can be obtained by the method of Lax–Wendroff [19,20], through applying it to transform the system of partial differential equations into a system of finite-difference equations. The scheme of the Lax–Wendroff method is a three-point explicit accuracy method comprising two steps: prediction and correction. It is easily applied to the resolution of conservative formulations [21]. The conservative formulation of Eqs. (1) to (4) writes as:

$$\frac{\partial Y}{\partial t} + \frac{\partial G(Y)}{\partial x} = H(Y) \tag{8}$$

F and H are two vector functions of the unknown vector Y defined by:

$$Y = \begin{pmatrix} u_x \\ v_x \\ u_t \\ v_t \end{pmatrix}, \qquad G = \begin{pmatrix} u_t \\ v_t \\ au_x + bv_x \\ bu_x + cv_x \end{pmatrix} \quad \text{and} \quad H = 0 \tag{9}$$

The spring is divided into N equal elements of length Δx. Indeed, with the notations of Fig. 2, we can write: $Y_i^k = Y[(i-1)\Delta x, k\Delta t]$ and $G_i^k = G(Y_i^k)$.

Moreover, the unknown vector $Y(x, t+\Delta t)$ can be approximated with the first terms of its Taylor expansion about t, as follows:

$$Y(x, t+\delta t) = Y\left((x,t) + \delta t \frac{\partial Y}{\partial t}\right) \tag{10}$$

Then, by introducing the physical laws of the dynamic response given by Eq. (8), i.e.:

$$\frac{\partial Y}{\partial t} = -\frac{\partial G(Y)}{\partial x} \tag{11}$$

we obtain the finite-difference form:

$$Y(x, t+\delta t) = Y(x,t) - \delta t \frac{\partial G}{\partial x} \tag{12}$$

Following the techniques described by Lerat and Peyret [22,23], the two-step Lax–Wendroff scheme used in conservative equation (8), for any grid point $(i, k+1)$, can be inferred from (12) and is as follows.

For the first step or prediction phase [instant $(k+1/2)\Delta t$]:

$$Y_{i+1/2}^{k+1/2} = \frac{1}{2}\left(Y_{i+1}^k + Y_i^k\right) - \frac{\Delta t}{2\Delta x}\left(G_{i+1}^k - G_i^k\right) \tag{13}$$

And for the second step or correction phase [instant $(k+1)\Delta t$]:

$$Y_i^{k+1} = Y_i^k - \frac{\Delta t}{\Delta x}\left(G_{i+1/2}^{k+1/2} - G_{i-1/2}^{k+1/2}\right) \tag{14}$$

where $\Delta x = h/N$ is the space division, N is the number of sections and Δt is the time division.

The finite-difference scheme of Lax–Wendroff is a three-point explicit method, of second-order accuracy. It can be shown that the requirement condition for stability is given by the Courant Friedrichs–Lewy condition:

$$\frac{\Delta t}{\Delta x} \leqslant \frac{1}{\max_k |\lambda_k|} \tag{15}$$

The λ_k are the eigenvalues of the matrix B, which is such that: $\frac{\partial G(Y)}{\partial x} = B\frac{\partial Y}{\partial x}$.

Under these conditions:

$$B = -\begin{bmatrix} 0 & a & 0 & b \\ 1 & 0 & 0 & 0 \\ 0 & b & 0 & c \\ 0 & 0 & 1 & 0 \end{bmatrix} \quad \text{and} \quad \det(B - \lambda I) = \lambda^4 - (a+c)\lambda^2 + \left(ac - b^2\right) = 0 \tag{16}$$

By posing $\mu = 1/\lambda$, Eq. (16) can be written as:

$$\left(ac - b^2\right)\mu^4 - (a+c)\mu^2 + 1 = 0 \tag{17}$$

which admits four roots: $\{-C_f, -C_s, C_s, C_f\}$ where C_f is the rapid angular wave celerity defined in the spring by:

$$C_f = \sqrt{\frac{(a+c) + \sqrt{(a-c)^2 + 4b^2}}{2}} = \sqrt{\frac{EIh}{Mr^2}\sin\alpha} \tag{18}$$

and

$$C_s = \sqrt{\frac{(a+c) - \sqrt{(a-c)^2 + 4b^2}}{2}} = \sqrt{\frac{EIh}{Mr^2}\frac{\sin\alpha}{1+\upsilon}} \tag{19}$$

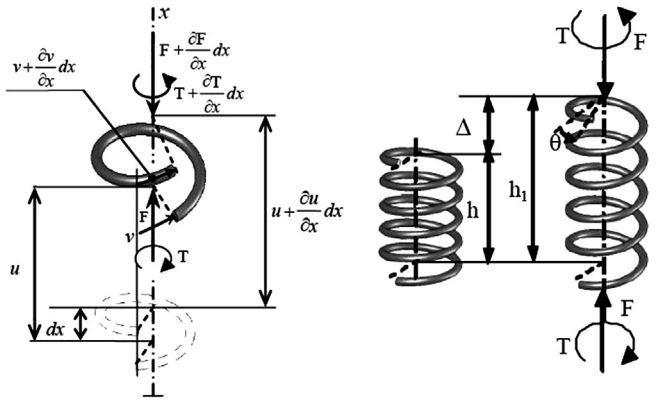

a. A spring element **b.** Static deformation of a helical spring

Fig. 1. Helical spring description.

Hence the stability condition can be written as:

$$\frac{\Delta t}{\Delta x} = \frac{1}{C_f} \tag{20}$$

The coefficients a, b and c can be expressed in terms of C_s:

$$\begin{cases} a = C_s^2\left(1 + \upsilon \sin^2 \alpha\right) \\ b = -C_s^2 \upsilon \cos\alpha \sin\alpha \\ c = C_s^2\left(1 + \upsilon \cos^2 \alpha\right) \end{cases} \tag{21}$$

Moreover, we can verify that:

$$a + c = C_s^2 + C_f^2 \quad \text{and} \quad ac - b^2 = C_s^2 C_f^2 \tag{22}$$

4. Impedance method

When the frequency varies in a certain interval, this method enables to determine the dynamic characteristics of the spring: frequency response, transfer function, etc. An analytical solution of the equations of motion can be obtained as algebraic equations in terms of mechanical and geometrical characteristics of the spring and boundary conditions. For this, the partial differential equations considered are linear; they are solved for sinusoidal perturbations with the same frequency throughout the system. The static behavior of the variables being initially zero ($\Delta = 0$ and $\theta = 0$), the instantaneous quantities are fluctuation terms.

It is advantageous to separate the total instantaneous mechanical variables (u_x, u_t, υ_x, υ_t) into two parts, the mean variables ($\bar{u}_x$, $\bar{u}_t$, $\bar{\upsilon}_x$, $\bar{\upsilon}_t$), and the oscillatory variables (u'_x, u'_t, υ'_x, υ'_t), so that ($u_x = \bar{u}_x + u'_x, \ldots$).

The mean variables are given by the initial conditions, represented by the static deflection of the spring (see Fig. 1b):

$$\bar{u}_x = -\frac{\Delta}{h}, \qquad \bar{u}_t = 0, \qquad \bar{\upsilon}_x = \frac{r\theta}{h}, \qquad \bar{\upsilon}_t = 0 \tag{23}$$

Using this notation, the equations of motion (1 to 4) become:

$$\frac{\partial u'_t}{\partial t} - a\frac{\partial u'_x}{\partial x} - b\frac{\partial \upsilon'_x}{\partial x} = 0 \tag{24}$$

$$\frac{\partial u'_x}{\partial t} - \frac{\partial u'_t}{\partial x} = 0 \tag{25}$$

$$\frac{\partial \upsilon'_t}{\partial t} - b\frac{\partial u_x}{\partial x} - c\frac{\partial \upsilon'_x}{\partial x} = 0 \tag{26}$$

$$\frac{\partial \upsilon'_x}{\partial t} - \frac{\partial \upsilon'_t}{\partial x} = 0 \tag{27}$$

As the behavior of the system is linear, Eqs. (24) to (27) have the same form as Eqs. (1) to (4). One may solve the linearized equations of the coupled free vibration of helical springs by using the separation-of-variables technique, which assumes that [10]:

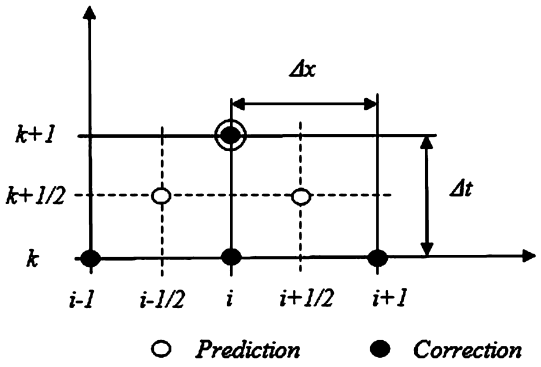

Fig. 2. Lax–Wendroff scheme.

$$\begin{aligned} u'_x &= u'_x(x,t) = U_x(x)T(t) \\ u'_t &= u'_t(x,t) = U_t(x)T(t) \\ \upsilon'_x &= \upsilon'_x(x,t) = V_x(x)T(t) \\ \upsilon'_t &= \upsilon'_t(x,t) = V_t(x)T(t) \end{aligned} \tag{28}$$

where $U_x(x)$, $V_x(x)$, $U_t(x)$ and $V_t(x)$ are non-time-varying complex functions of strains and velocities, and T is a function of t only.

The impedance method [10] consists in solving the equations of system (8) by the method of separation of variables $Y(x,t) = X(x)T(t)$, where $X^t(x) = (\,U_x\ V_x\ U_t\ V_t\,)$ a vector of the single variable x and T is a function of the single variable t.

By restricting the solution for T to the steady-oscillatory case, that is, by assuming a particular solution for T as a harmonic oscillation, the solution can be expressed as:

$$T(t) = De^{st} \tag{29}$$

where s is a complex-valued constant independent of space x and time t. s constant, is referred as the complex frequency, or the Laplace variable, contains real and imaginary part σ and ω, respectively ($s = \sigma + i\omega$). The constant γ ($\gamma = \alpha + i\delta$), which is a function of s, is called "the propagation constant". The real parts of γ and s govern the decay of oscillations with respect to time at a particular section and the attenuation of oscillations over a distance, respectively. The solution of X is then of the form: $X = Ae^{\gamma x} + Be^{-\gamma x}$. Where A and B are constants of integration.

If we assume that the damping is negligible in the spring ($\sigma = 0$). Can therefore simplified solution and remains only the imaginary part ($s = i\omega$).

After substituting and rearranging:

$$\frac{\mathrm{d}X}{\mathrm{d}x} = i\omega B^{-1}X \tag{30}$$

where:

$$X(x) = \begin{bmatrix} U_x \\ V_x \\ U_t \\ V_t \end{bmatrix}, \qquad B = \begin{bmatrix} 0 & 0 & 1 & 0 \\ 0 & 0 & 0 & 1 \\ a & b & 0 & 0 \\ b & c & 0 & 0 \end{bmatrix} = \begin{bmatrix} 0 & 0 & 1 & 0 \\ 0 & 0 & 0 & 1 \\ C_s^2(1+\upsilon\sin^2\alpha) & -C_s^2\upsilon\sin\alpha\cos\alpha & 0 & 0 \\ -C_s^2\upsilon\sin\alpha\cos\alpha & C_s^2(1+\upsilon\cos^2\alpha) & 0 & 0 \end{bmatrix}$$

the solution of Eq. (30) can be written as [25,26]:

$$X(x) = \mathrm{e}^{i\omega x B^{-1}}X(0) = \big[A(x)\big]X(0) \tag{31}$$

The inverse of matrix B can be easily found by the Gauss elimination method:

$$B^{-1} = \begin{bmatrix} 0 & 0 & \frac{c}{ac-b^2} & \frac{-b}{ac-b^2} \\ 0 & 0 & \frac{-b}{ac-b^2} & \frac{a}{ac-b^2} \\ 1 & 0 & 0 & 0 \\ 0 & 1 & 0 & 0 \end{bmatrix} = \begin{bmatrix} 0 & 0 & \frac{1+\upsilon\cos^2\alpha}{C_f^2} & \frac{\upsilon\sin\alpha\cos\alpha}{C_f^2} \\ 0 & 0 & \frac{\upsilon\sin\alpha\cos\alpha}{C_f^2} & \frac{1+\upsilon\sin^2\alpha}{C_f^2} \\ 1 & 0 & 0 & 0 \\ 0 & 1 & 0 & 0 \end{bmatrix} \tag{32}$$

The eigenvalues of B^{-1} are the roots of the characteristic equation:

$$\det\left(B^{-1}-\lambda I\right)=\lambda^4-\frac{a+c}{ac-b^2}\lambda^2+\frac{1}{ac-b^2}=0 \tag{33}$$

This equation has four roots, which are:

$$\lambda=\pm\sqrt{\frac{(a+c)\pm\sqrt{(a-c)^2+4b^2}}{2(ac-b^2)}} \tag{34}$$

Substituting expressions (5) to (7) into Eq. (34) yields:

$$\lambda_1=-\sqrt{\frac{Mr^2}{EIH}\frac{(1+\upsilon)}{\sin\alpha}}=-\frac{1}{C_s},\quad \lambda_2=-\sqrt{\frac{Mr^2}{EIH}\frac{1}{\sin\alpha}}=-\frac{1}{C_f},\quad \lambda_3=\sqrt{\frac{Mr^2}{EIH}\frac{1}{\sin\alpha}}=\frac{1}{C_f}\quad\text{and}$$
$$\lambda_4=\sqrt{\frac{Mr^2}{EIH}\frac{(1+\upsilon)}{\sin\alpha}}=\frac{1}{C_s} \tag{35}$$

Since B^{-1} is a four-by-four matrix, then, from the algebraic theory, Eq. (31) can be written as [24]:

$$X(x)=\left[A(x)\right]X(0)=\left[a_0I+a_1\left(i\omega xB^{-1}\right)+a_2\left(i\omega xB^{-1}\right)^2+a_3\left(i\omega xB^{-1}\right)^3\right]X(0) \tag{36}$$

where a_r values are defined by using determinants: $a_r=\frac{D_r}{D}$, with:

$$D=\begin{vmatrix}1 & 1 & 1 & 1\\ i\omega x\lambda_1 & i\omega x\lambda_2 & i\omega x\lambda_3 & i\omega x\lambda_4\\ (i\omega x\lambda_1)^2 & (i\omega x\lambda_2)^2 & (i\omega x\lambda_3)^2 & (i\omega x\lambda_4)^2\\ (i\omega x\lambda_1)^3 & (i\omega x\lambda_2)^3 & (i\omega x\lambda_3)^3 & (i\omega x\lambda_4)^3\end{vmatrix}=-4\upsilon^2\sqrt{1+\upsilon}\left(\frac{\omega x}{C_f}\right)^6 \tag{37}$$

D_r is obtained by replacing the elements$(i\omega x\lambda_1)^r,\ldots,(i\omega x\lambda_4)^r$ in D bye$^{i\omega x\lambda_1},\ldots,\mathrm{e}^{i\omega x\lambda_4}$.

The eigenvalues of matrix B are $\{-C_f,-C_s,C_s,C_f\}$ and those of the matrix $ix\omega B^{-1}$ are $\{\lambda_1=-i\omega x/C_s,\lambda_2=-i\omega x/C_f,\lambda_3=i\omega x/C_f,\lambda_4=i\omega x/C_s\}$.

By using Mathematica processing software, the following coefficients of the matrix $[A(x)]$, indicated in the relation (33), are obtained:

$$A_{11}=A_{33}=\sin^2\alpha\cos\left(\frac{\omega x}{C_f}\right)+\cos^2\alpha\cos\left(\frac{\omega x}{C_s}\right) \tag{38}$$

$$A_{12}=A_{21}=A_{34}=A_{43}=\sin\alpha\cos\alpha\left[\cos\left(\frac{\omega x}{C_s}\right)-\cos\left(\frac{\omega x}{C_f}\right)\right] \tag{39}$$

$$A_{13}=i\frac{\sin^2\alpha}{C_f}\sin\left(\frac{\omega x}{C_f}\right)+i\frac{\cos^2\alpha}{C_s}\sin\left(\frac{\omega x}{C_s}\right) \tag{40}$$

$$A_{14}=A_{23}=-i\sin\alpha\cos\alpha\left[\frac{1}{C_f}\sin\left(\frac{\omega x}{C_f}\right)-\frac{1}{C_s}\sin\left(\frac{\omega x}{C_s}\right)\right] \tag{41}$$

$$A_{22}=A_{44}=\cos^2\alpha\cos\left(\frac{\omega x}{C_f}\right)+\sin^2\alpha\cos\left(\frac{\omega x}{C_s}\right) \tag{42}$$

$$A_{24}=i\frac{\cos^2\alpha}{C_f}\sin\left(\frac{\omega x}{C_f}\right)+i\frac{\sin^2\alpha}{C_s}\sin\left(\frac{\omega x}{C_s}\right) \tag{43}$$

$$A_{31}=iC_f\sin^2\alpha\sin\left(\frac{\omega x}{C_f}\right)+iC_s\cos^2\alpha\sin\left(\frac{\omega x}{C_s}\right) \tag{44}$$

$$A_{32}=A_{41}=i\cos\alpha\sin\alpha\left[C_s\sin\left(\frac{\omega x}{C_s}\right)-C_f\sin\left(\frac{\omega x}{C_f}\right)\right] \tag{45}$$

$$A_{42}=iC_f\cos^2\alpha\sin\left(\frac{\omega x}{C_f}\right)+iC_s\sin^2\alpha\sin\left(\frac{\omega x}{C_s}\right) \tag{46}$$

Hence, the complex strains and velocities, as functions of position x in the helical spring, are:

$$\begin{aligned}U_x(x)&=A_{11}(x)U_x(0)+A_{12}(x)V_x(0)+A_{13}(x)U_t(0)+A_{14}(x)V_t(0)\\ V_x(x)&=A_{21}(x)U_x(0)+A_{22}(x)V_x(0)+A_{23}(x)U_t(0)+A_{24}(x)V_t(0)\\ U_t(x)&=A_{31}(x)U_x(0)+A_{32}(x)V_x(0)+A_{33}(x)U_t(0)+A_{34}(x)V_t(0)\\ V_t(x)&=A_{41}(x)U_x(0)+A_{42}(x)V_x(0)+A_{43}(x)U_t(0)+A_{44}(x)V_t(0)\end{aligned} \tag{47}$$

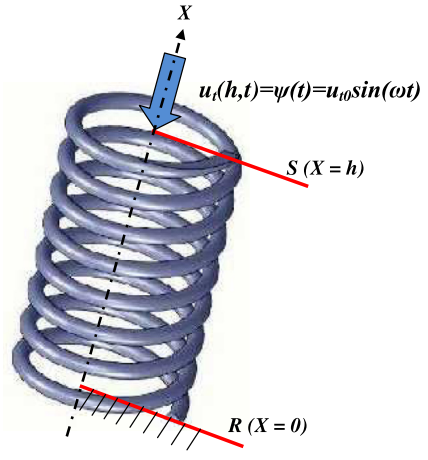

Fig. 3. Ends of the helical spring fixed at R ($x=0$) and subjected to axial loading at S ($x=h$).

It can be noted that:

$$A_{ij}(0)=\delta_{ij} \tag{48}$$

The mechanical impedances in the helical spring are defined as the ratio of complex axial and angular strains to the complex axial and angular velocities, as follows:

$$\begin{aligned}
Z_1(x)&=\frac{u_x'}{u_t'}=\frac{A_{11}(x)U_x(0)+A_{12}(x)V_x(0)+A_{13}(x)U_t(0)+A_{14}(x)V_t(0)}{A_{31}(x)U_x(0)+A_{32}(x)V_x(0)+A_{33}(x)U_t(0)+A_{34}(x)V_t(0)}\\
Z_2(x)&=\frac{\upsilon_x'}{u_t'}=\frac{A_{21}(x)U_x(0)+A_{22}(x)V_x(0)+A_{23}(x)U_t(0)+A_{24}(x)V_t(0)}{A_{31}(x)U_x(0)+A_{32}(x)V_x(0)+A_{33}(x)U_t(0)+A_{34}(x)V_t(0)}\\
Z_1'(x)&=\frac{u_x'}{\upsilon_t'}=\frac{A_{11}(x)U_x(0)+A_{12}(x)V_x(0)+A_{13}(x)U_t(0)+A_{14}(x)V_t(0)}{A_{41}(x)U_x(0)+A_{42}(x)V_x(0)+A_{43}(x)U_t(0)+A_{44}(x)V_t(0)}\\
Z_2'(x)&=\frac{\upsilon_x'}{\upsilon_t'}=\frac{A_{21}(x)U_x(0)+A_{22}(x)V_x(0)+A_{23}(x)U_t(0)+A_{24}(x)V_t(0)}{A_{41}(x)U_x(0)+A_{42}(x)V_x(0)+A_{43}(x)U_t(0)+A_{44}(x)V_t(0)}
\end{aligned} \tag{49}$$

Since the mechanical system has four degree of freedom, the transfer functions in the spring are defined as the ratio of the complex angular strain or velocity to the complex axial strain or velocity, respectively:

$$W_1(x)=\frac{\upsilon_x'}{u_x'}=\frac{A_{21}(x)U_x(0)+A_{22}(x)V_x(0)+A_{23}(x)U_t(0)+A_{24}(x)V_t(0)}{A_{11}(x)U_x(0)+A_{12}(x)V_x(0)+A_{13}(x)U_t(0)+A_{14}(x)V_t(0)}$$

and

$$W_2(x)=\frac{\upsilon_t'}{u_t'}=\frac{A_{41}(x)U_x(0)+A_{42}(x)V_x(0)+A_{43}(x)U_t(0)+A_{44}(x)V_t(0)}{A_{31}(x)U_x(0)+A_{32}(x)V_x(0)+A_{33}(x)U_t(0)+A_{34}(x)V_t(0)} \tag{50}$$

In practice, we are interested in the mechanical impedances at the extremity S($x=h$) of the spring, as indicated in Fig. 3.

In the case where the spring is clamped at the extremity R($x=0$) and axially loaded at the extremity S, the boundary conditions can be expressed as:

$$U_t(0)=0 \qquad V_t(0)=0 \qquad U_t(h)\neq 0 \qquad V_t(h)=0 \tag{51}$$

Impedance transfer functions are utilized to express the impedance at one point in terms of conditions at another location, usually a terminal condition. For example, at $x=0$, $W_1(0)=V_x(0)/U_x(0)$. Although transfer functions may be written to relate the impedance at any position x in a spring to the boundary conditions, the transfer equation that relates impedance at the loaded extremity in terms of impedance at the clamped extremity is particularly useful:

$$Z_1(h)=\frac{A_{11}(h)+W_1(0)A_{12}(h)}{A_{31}(h)+W_1(0)A_{32}(h)} \quad \text{and} \quad Z_2(h)=\frac{A_{21}(h)+W_1(0)A_{22}(h)}{A_{31}(h)+W_1(0)A_{32}(h)} \tag{52}$$

From relations (54), $V_t(h)=0$ leads to:

$$W_1(0)=\frac{V(0)}{U(0)}=-\frac{A_{41}(h)}{A_{42}(h)} \tag{53}$$

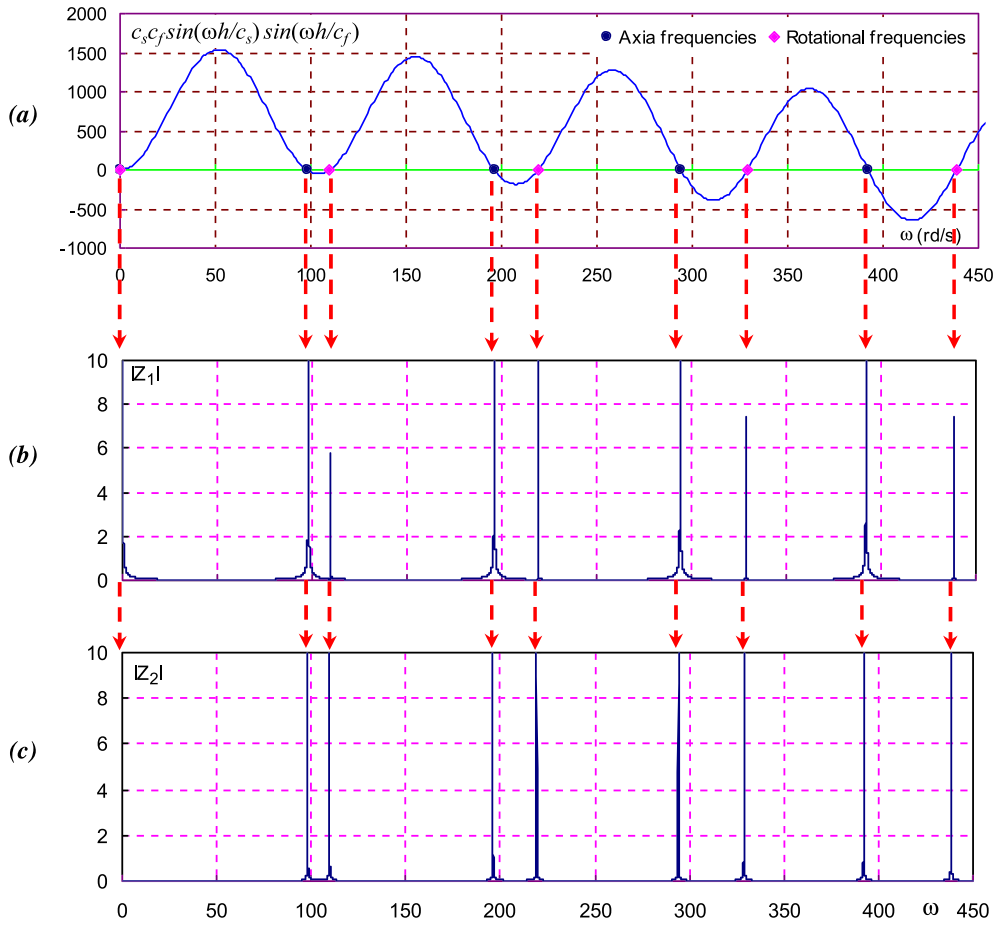

Fig. 4. Correspondence between the natural frequencies of the helical spring at $x = h$ (a) and the impedence diagrams (b), (c). Color online.

Under these conditions, the impedance formulas, at $x = h$, are simplified:

$$Z_1(h) = \frac{A_{11}(h)A_{42}(h) - A_{12}(h)A_{41}(h)}{A_{31}(h)A_{42}(h) - A_{32}(h)A_{41}(h)} \quad \text{and} \quad Z_2(h) = \frac{A_{21}(h)A_{42}(h) - A_{22}(h)A_{41}(h)}{A_{31}(h)A_{42}(h) - A_{32}(h)A_{41}(h)} \tag{54}$$

In the case where the load is angular, one can define two others impedances at the loaded extremity:

$$Z'_1(h) = \frac{A_{11}(h) + W_1(0)A_{12}(h)}{A_{41}(h) + W_1(0)A_{42}(h)} \quad \text{and} \quad Z'_2(h) = \frac{A_{21}(h) + W_1(0)A_{22}(h)}{A_{41}(h) + W_1(0)A_{42}(h)} \tag{55}$$

where, from relations (47), $U_t(h) = 0$ leads to:

$$W_1(0) = -\frac{A_{31}(h)}{A_{32}(h)} \tag{56}$$

and the impedances at $x = h$ are simplified:

$$Z'_1(h) = \frac{A_{11}(h)A_{32}(h) - A_{12}(h)A_{31}(h)}{A_{41}(h)A_{32}(h) - A_{42}(h)A_{31}(h)} \quad \text{and} \quad Z'_2(h) = \frac{A_{21}(h)A_{32}(h) - A_{22}(h)A_{31}(h)}{A_{41}(h)A_{32}(h) - A_{42}(h)A_{31}(h)} \tag{57}$$

The impedances (54) vary with the frequency and are maximal for an infinite number of frequencies. These are the natural frequencies of the helical spring system and they correspond to the zero of the impedance denominator, i.e. the zero of expression (Fig. 4):

$$A_{41}(h)A_{32}(h) - A_{31}(h)A_{42}(h) \tag{58}$$

The amplitudes of the two impedances (57) according to the pulse diagrams are shown in the impedance diagrams (Fig. 4). The maximum values of the spectrum are on resonance frequencies, while the minimum values correspond

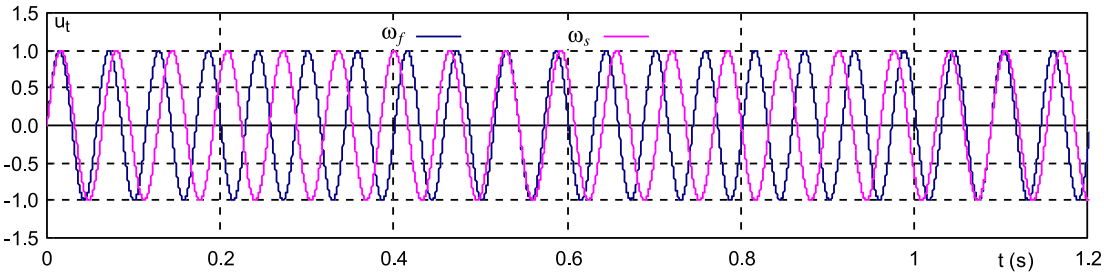

Fig. 5. Sinusoidal excitation of the axial velocity at the impacted end of the spring $x = h$. Color online.

Table 1
Mechanical and geometric characteristics of the considered springs.

Height of the spring	h	1193.8 mm
Helix angle	α	0.198281 rad
Number of turns	n	6
Poisson's ratio	υ	0.25
Young's modulus	E	206.85 GPa
Mass of the spring	M	2.12868 kg
Radius of the spring	r	157.607 mm
Wire radius	r_f	7 mm
Initial compression	Δ	254 mm

to anti-resonance frequencies. When the pulse perturbations in the spring coincide with the resonance pulsations, strain fluctuations are amplified and can cause the breakage of the spring. Several numerical methods can be used to determine these fluctuations [25].

The following application illustrates the steps in a frequency response analysis, in which the impedance method is used. The computations needed to evaluate the mechanical impedances at a point in a spring are quite involved when a computer is not used. The general applicability of the method can be best indicated by discussing particular situations. In the following examples, the receiving-end impedance of the system is assumed definable by the foregoing relationships, the problem being to determine the impedance at other locations in the system.

5. Applications and results

5.1. Initial conditions

The spring is initially compressed at a distance Δ (see Fig. 1). For all $x \in [0, h]$, the initial conditions are defined by:

$$u_x(x,0) = -\Delta/h, \qquad v_x(x,0) = \theta r/h = 0, \qquad u_t(x,0) = 0 \quad \text{and} \quad v_t(x,0) = 0 \tag{59}$$

These conditions satisfy the ordinary differential equation system obtained after having annulled terms $\partial/\partial t$ in partial differential equations described by (1), (2), (3) and (4).

5.2. Boundary conditions

Consider a system spring shown in Fig. 3. The boundary conditions are expressed by:

$$u_t(0,t) = 0, \qquad v_t(0,t) = 0, \qquad u_t(h,t) = \psi(t) = u_{t0}\sin(\omega t) \quad \text{and} \quad v_t(h,t) = 0 \tag{60}$$

The dynamic response studied here is due to sinusoidal excitations of the axial velocity at the end of the spring $x = h$. Fig. 6 shows the excitation with the fundamentals frequencies. A FORTRAN program was run on a PC computer. The problem has been solved by the finite difference Lax–Wendroff method using $N = 200$ grid points. The dynamic behaviour of the spring is represented by axial waves and induced rotational waves because the coupling effect of Poisson. The coupling effect may be accompanied with beating phenomena.

5.3. System description

Consider a system of steel helical spring whose geometric and mechanical characteristics are shown in Table 1.

A computer program in Fortran language has been developed, which computes the mechanical impedances over a wide range of frequencies ω. In general, the terminal impedances are complex numbers and can be expressed as:

$$Z_1(h) = Z_{1R} + iZ_{1I} = |Z_1|e^{i\psi_1} \quad \text{and} \quad Z_2(h) = Z_{2R} + iZ_{2I} = |Z_2|e^{i\psi_2} \tag{61}$$

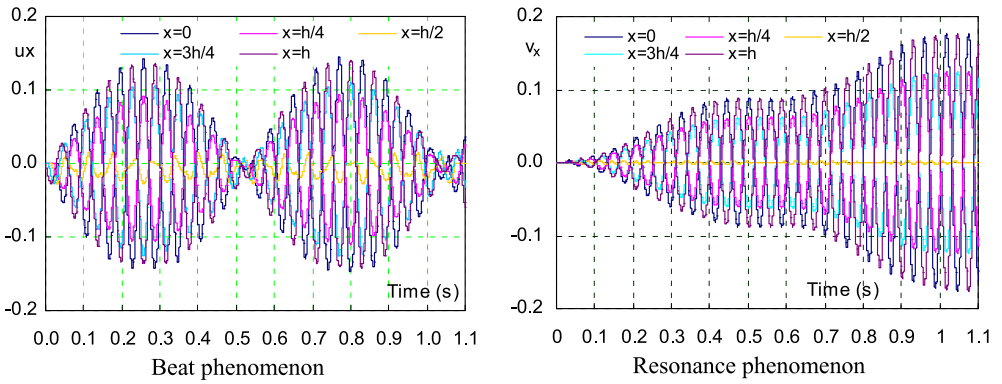

Fig. 6. Evolution of deformation following an excitation at the rapid fundamental period ω_f. Color online.

Theses impedances vary with frequency and are maximal for an infinite number of resonating frequencies. These are the natural frequencies of the helical spring system and, in the case of a spring originating in a clamped extremity, they correspond to fundamental and harmonics. Each natural frequency or resonance, however, is separated on the frequency scale by an anti-resonance, or frequency at which $|Z_1|$ and $|Z_2|$ become small or equal zero.

The impedance diagram provides a very useful aid in assessing the frequency response of a system. The most useful plot is that of the modulus of the impedance versus the angular frequency. The impedance diagrams for the helical spring are shown in Fig. 5, where the impedance modulus is plotted.

The resonances and anti-resonances are visible as points of high impedance and low impedance, respectively. The fundamental, second, third and fourth harmonics are easily identified as the frequencies associated with large impedances. These frequencies correspond to the maximum impedance modulus values, that is, to the resonance frequencies and are proportional to C_s and C_f, respectively. The two fundamental frequencies are given by:

$$\omega_s = \frac{\pi \cdot C_s}{h} = 98.035 \text{ rad/s} \quad \text{and} \quad \omega_f = \frac{\pi \cdot C_f}{h} = 109.607 \text{ rad/s} \tag{62}$$

The corresponding natural fundamental frequencies, expressed in Hz, are:

$$f_s = \frac{\omega_s}{2\pi} = \frac{C_s}{2h} = 15.60 \text{ Hz} \quad \text{and} \quad f_f = \frac{\omega_f}{2\pi} = \frac{C_f}{2h} = 17.44 \text{ Hz} \tag{63}$$

As indicated in Fig. 5, the number series of natural frequencies correspond to the zero of the denominator of $|Z_1|$ and $|Z_2|$, that is the zero of expression (58). The others natural frequencies are the multiples of ω_s and ω_f:

$$\omega_{sk} = k\frac{\pi \cdot C_s}{h} = 98.035k, \quad \omega_{fk} = k\frac{\pi \cdot C_f}{h} = 109.607k, \quad k = 0\ 1\ 2\ \ldots \tag{64}$$

5.4. Excitation with fast frequency ω_f

The numerical results are shown in Fig. 6, which illustrates the dynamic response represented by the forced vibration of the strains in the spring. This dynamic response in different sections of the spring is due to a sinusoidal excitation of the axial velocity of amplitude 1 m/s and of pulse corresponding to the fundamental frequency $\omega_f = \frac{\pi \cdot C_f}{h} = 109.607$ rad/s, i.e. to the faster wave celerity.

The evolutions of axial and rotational strains, as functions of time t, are plotted at some sections of the spring: $x = 0$, $x = h/4$, $x = h/2$, $x = 3h/4$, and $x = h$. From these results, the strains are maximal at the extremities of the spring.

Note that the resonance phenomenon occurs for the angular deformation, because the pulse ω_f is a fundamental to this mechanical quantity. Therefore, it is amplified continuously until it reaches a steady oscillatory regime. One can notice that the angular deformation is maximal at both ends of the spring. For the axial deformation, it is rather a wave beat phenomenon that occurs. Again, the deformation is maximal at both ends of the spring. The observed beat phenomenon develops when two signals of the same type are energized with close frequencies. In this case, it is the axial velocity of the wave that grows with an excitation pulse of $\omega_f = 109.607$ rad/s, and the axial strain wave which is excited with the slow pulse $\omega_s = 98.035$ rad/s. So, the beat phenomenon reveals two characteristic times: $T_0 = \frac{4\pi}{\omega_{s1}+\omega_{f1}} = 0.0605$ s and $T_b = \frac{2\pi}{|\omega_{f1}-\omega_{s1}|} = 0.543$ s.

T_0, which is proportional to the inverse of the mean pulse waves, corresponds to the period of the oscillations of the resulting signal and T_b, which is proportional to the difference between pulse waves, represents the period of the envelope of these oscillations, that is the period of the beat or of the modulation. Actually, the resonance phenomenon can not be developed for axial waves with fast beat, as they are quickly caught and then destroyed by the angular wave [19].

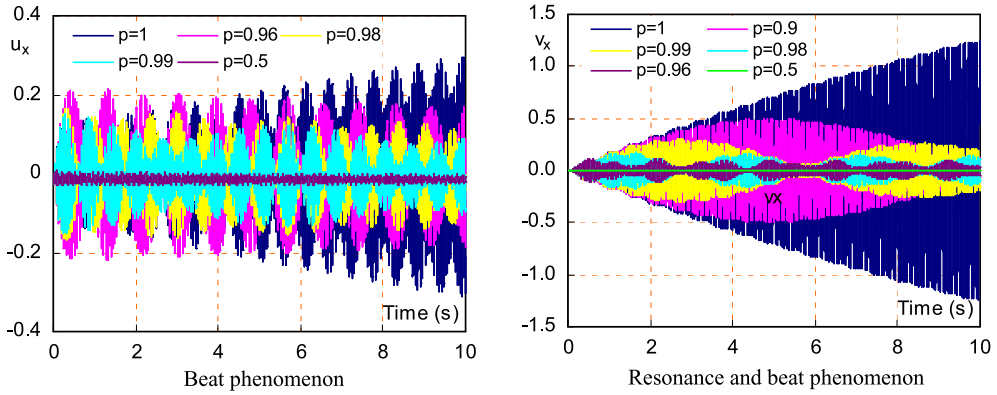

Fig. 7. Evolution of deformation at $x = h$ for different values of the frequency. Color online.

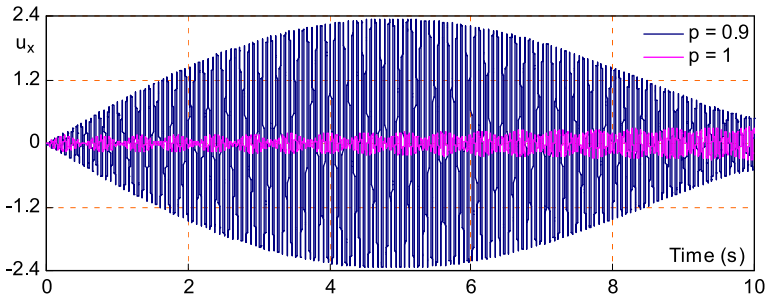

Fig. 8. Amplification of the beat of the axial deformation at $x = h$. Color online.

It can be seen that the resonance phenomenon manifests for rotational strains at all sections only at the middle of the spring $x = h/2$. For the axial strain, the resonance is reduced to the beat phenomenon that takes place between the two waves: the excitation u_t which fluctuates at the fast frequency and the axial strain u_x, which propagates at the slow wave celerity. This can be explained by the fact that the excitation frequency is equal to the fundamental frequency of the rapid rotational waves. Although the excitation frequency is also a fundamental for the axial strain, the resonance of this strain did not occur, due the coupling effect and the competition of the axial and rotational waves.

Fig. 7 shows the response of the spring in terms of axial and angular deformation for several values of the frequency. Coefficient p is the ratio of the excitation frequency ω to the fast fundamental frequency ω_f:

$$p = \frac{\omega}{\omega_f} \tag{65}$$

Note that the curve giving the evolution of the axial strain corresponding to $p = 0.9$ has not been traced, because for this value, the excitation frequency is close enough to the slow fundamental pulse ω_{s1} and causes a very amplified beat of the axial strain, as shown in Fig. 8.

5.5. Excitation with slow frequency ω_s

Fig. 9 shows the evolution of axial and angular deformations due to a sinusoidal excitation to the axial velocity with the natural frequency of the slow speed. The results show that the axial strain is increasing continuously, and significantly reflects the growing resonance phenomenon in the spring for this quantity. The results also show that the resonance phenomenon expands to the angular deformation. This can be explained by the dynamic coupling between the axial waves and angular waves reflecting the fact that the angular waves are induced in the spring by the axial waves and are never caught by these waves.

However, as shown in Fig. 10, the amplification in this case is slightly higher despite the slow frequency $f_s = \frac{1}{T_s} = \frac{\omega_s}{2\pi} = 15.603$ Hz is smaller than the fast frequency $f_f = \frac{1}{T_f} = \frac{\omega_f}{2\pi} = 17.445$ Hz.

In Fig. 11, the responses of the spring, in terms of angular and axial strains, are shown for several values of the frequency. The coefficient p is the ratio of the excitation frequency ω and of the slow fundamental frequency ω_s:

$$q = \frac{\omega}{\omega_s} \tag{66}$$

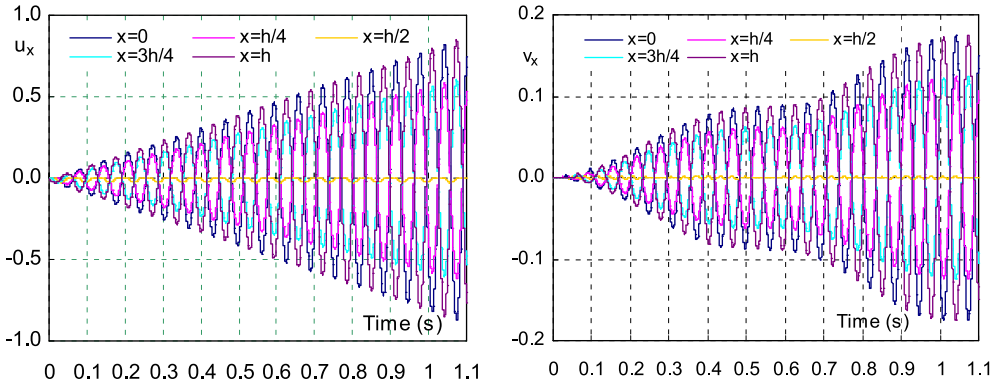

Fig. 9. Evolution of deformation following an excitation at the fundamental period of slow ω_s. Color online.

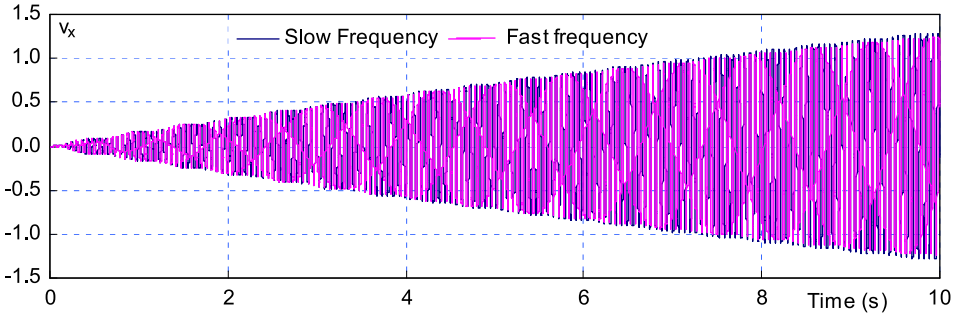

Fig. 10. Evolution of the angular deformation at $x = h$ for two frequencies. Color online.

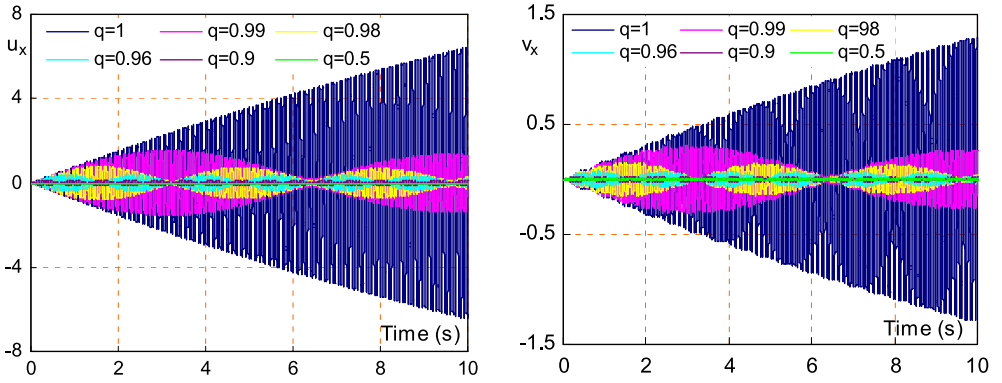

Fig. 11. Evolution of deformation at $x = h$ for different values of the frequency. Color online.

The resonance of a system is a phenomenon that may be initiated very gradually and that builds up a steady-oscillatory flow (unless failure occurs). If a forcing action is applied, resonance will develop and take the forcing function period if it is close to the fundamental or a harmonic period of the system. When a system is altered from static conditions by a periodic forcing function, a beat of transitory nature occurs if the forcing period is not the fundamental or harmonic of the system.

5.6. Excitation with harmonic frequencies

Fig. 12 presents dynamic responses of the spring in term of axial and rotational strains due to an excitation in the axial velocity $u_t(h) = \sin(\omega t)$. Different harmonics of the two fundamental spring frequencies, $\omega = k\omega_s$ and $\omega = k\omega_f$ were used. These results are obtained by the method of Lax–Wendroff and are drawn at the end $x = h$ of the spring. As it can be seen on these figures, the resonance phenomenon occurs at axial and rotational strains for all harmonics corresponding to the slow frequency ω_s. Similarly, it is confirmed that the beat phenomenon occurs for the axial strain when harmonics correspond the fast frequency ω_f. Moreover, as shown in Fig. 13, the phenomenon of resonance of rotational strain occurs for all harmonics corresponding to this fast frequency. We can clearly observe that the resonance and the beat proceed in stages or by levels for both axial and rotational strains and these are very clear for high harmonics. That is, for the

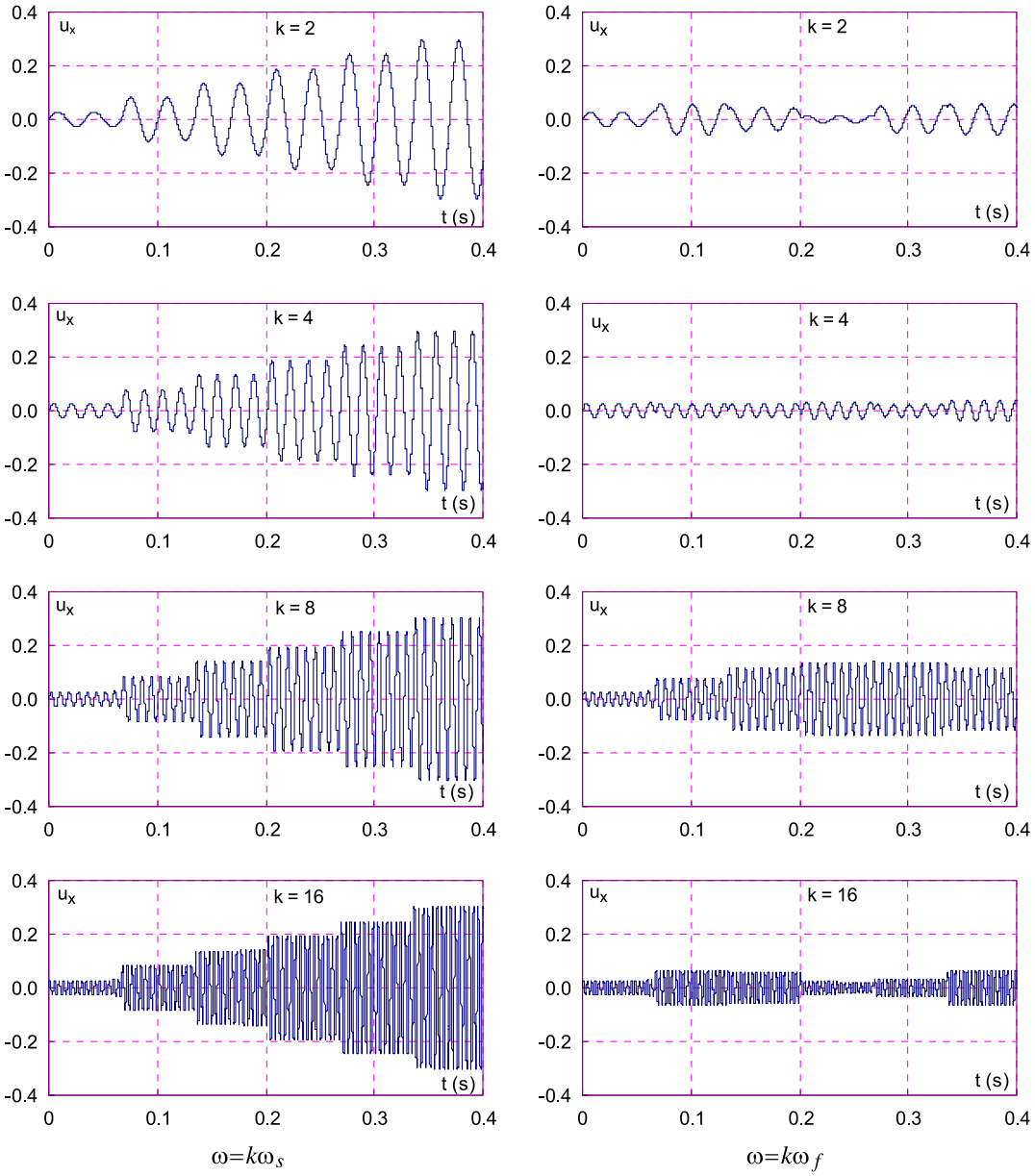

Fig. 12. Evolution of the axial strain at $x = h$ due to a sinusoidal excitation of u_t at harmonic frequency of order k.

harmonic of order k, the amplitude of the axial strain corresponding to the slow excitation frequency remains constant every k periods. The same effect is observed for excitation with fast frequency harmonic. Fig. 14 shows the evolution of the strains, at $x = h$, obtained for different harmonics and presented for more important time period. It can be seen that the evolution in stages of stains shows a loss in their amplitude modulation. This amortization is more pronounced for higher harmonics.

6. Conclusion

This paper investigated the resonance and beat phenomena of strains due to forced sinusoidal excitation in helical springs. To study vibrations in helical springs subjected to a sinusoidal excitation, we propose a coupled model. At first, the natural frequencies of the spring were predicted by the impedance method. The impedance approach has been used by restricting the solution to the steady oscillatory case, that is, by assuming harmonic oscillations. In this case, as the behavior of the mechanical variables was governed by a linear system of partial differential equations, the separation of variables technique has been used to develop the mechanical impedances of the spring. Theses impedances vary with frequency and are maximal for the infinite number of resonating frequencies corresponding to fundamental and harmonics.

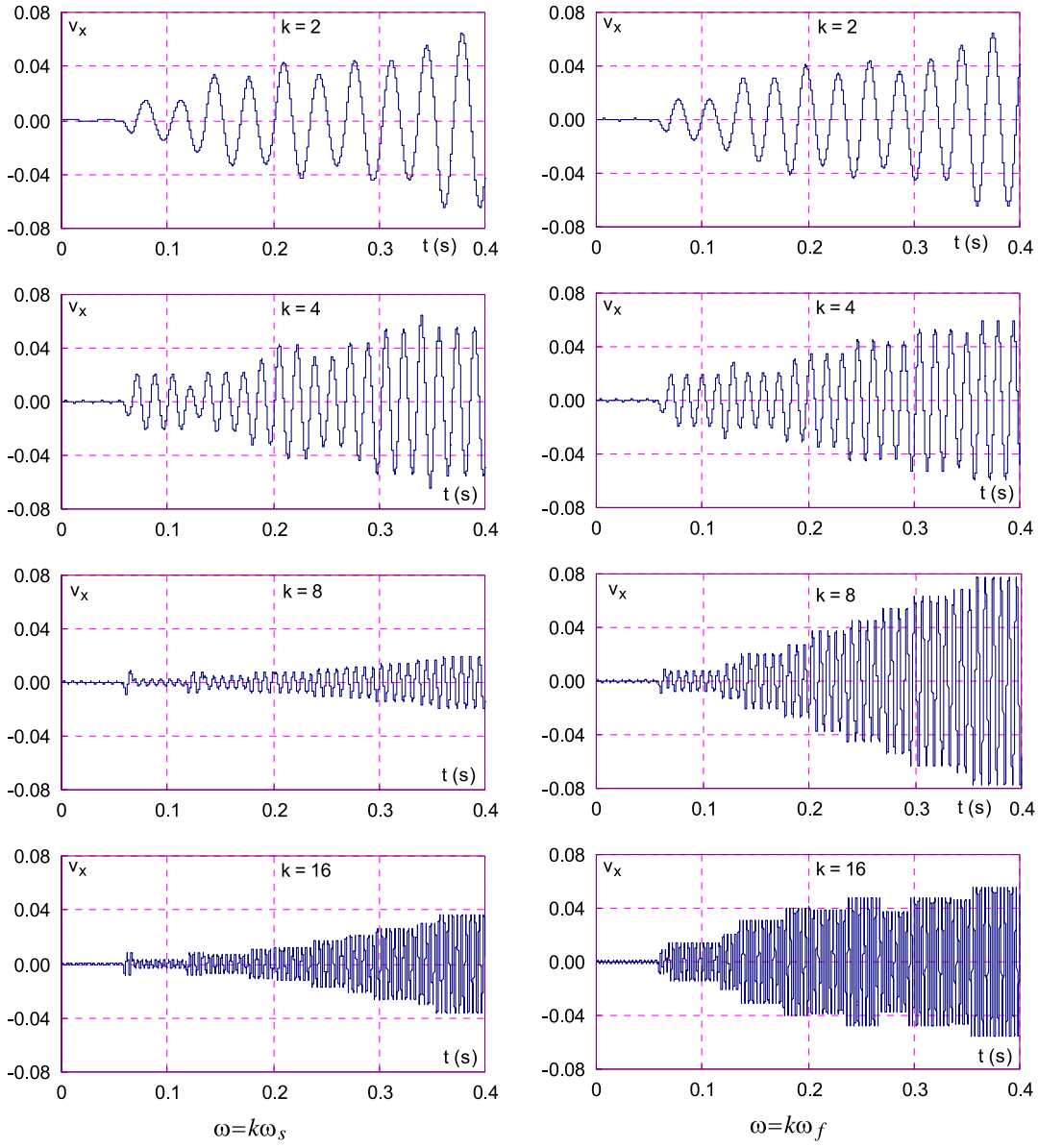

Fig. 13. Evolution of the rotational strain at $x = h$ due to a sinusoidal excitation of u_t at harmonic frequency of order k.

The obtained results permitted to show that the natural frequencies are proportional to the two wave speeds in the spring: the slow axial wave speed and the rapid rotational wave speed. Next, the evolution of axial and rotational strains, at various sections of the spring, due to an axial velocity harmonic excitation, was analyzed and the phenomenon of resonance and beat was illustrated. Numerical solutions were obtained by the Lax–Wendroff scheme when the vibrations were caused by harmonic forced axial velocity. As there were two different sets of natural frequencies, because of the two different waves that propagated through the spring, the dynamic behavior of the strains was conditioned by the wave that matched the frequency of the excitation when resonance occurred. In this sense, our numerical results showed that the axial and rotational strains resonated and followed the excitation for slow frequencies. The amplification is more important for the axial deformation than for the angular deformation, which was resulting from the effect of coupling Poisson. Numerical results related to the studied and simulated example have been confronted with such physical explanations regarding the dynamical coupling between the axial and angular waves and the phenomena of wave reflections on both ends of the spring. For excitations with rapid natural frequencies, the resonance occurred only for rotational strains and the beat phenomenon was observed for axial strain.

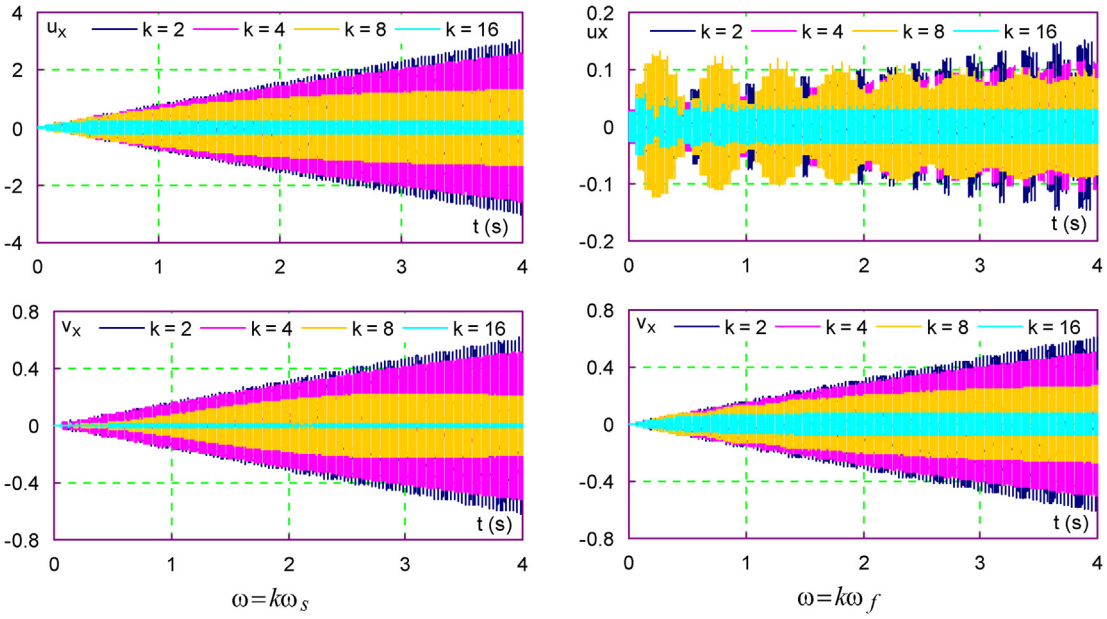

Fig. 14. Effect of the harmonic frequency order on resonance or beat amortizations.

References

[1] A.M. Wahl, Mechanical Springs, Penton Publishing Co., Cleveland, Ohio, 1963.
[2] W.H. Wittrick, On elastic wave propagation in helical springs, Int. J. Mech. Sci. 8 (1966) 25–47.
[3] A.E.H. Love, A Treatise on the Mathematical Theory of Elasticity, 4th edition, Dover Publications, New York, 1927.
[4] F. Dammak, M. Taktak, S. Abid, A. Dhieb, M. Haddar, Finite element method for the stress analysis of isotropic cylindrical helical spring, Eur. J. Mech. A, Solids 24 (12) (2005) 1068–1078.
[5] Y. Kagawa, On the dynamical properties of helical springs of finite length with small pitch, J. Sound Vib. 8 (1) (1968) 1–15.
[6] M. Duchemin, Ressorts soumis à une force coaxiale, Tech. Ing. BD3 B 5435 (1986) 1–23.
[7] V.K. Stokes, On the dynamic radial expansion of helical springs due to longitudinal impact, J. Sound Vib. 35 (1974) 77.
[8] B. Gironnet, G. Louradour, Comportement dynamique des ressorts, Tech. Ing. BD2 (1983) B610-1–B610-11.
[9] V. Yildirim, Expressions for predicting fundamental natural frequencies of non-cylindrical helical springs, J. Sound Vib. 252 (3) (2002) 479–491.
[10] E.B. Wylie, V.L. Streeter, L. Suo, Fluid Transients in Systems, Prentice Hall, Englewood Cliffs NJ, 1993.
[11] V. Yildirim, An efficient numerical method for predicting the natural frequencies of cylindrical helical springs, Int. J. Mech. Sci. 41 (1999) 919–939.
[12] J. Lee, D.J. Thompson, Dynamic stiffness formulation, free vibration and wave motion of helical springs, J. Sound Vib. 239 (2) (2001) 279–320.
[13] L. Lee, Free vibration analysis of cylindrical helical springs by the pseudo spectral method, J. Sound Vib. 302 (2007) 185–196.
[14] L.E. Becker, G.G. Chassie, W.L. Cleghorn, On the natural frequencies of helical compression springs, Int. J. Mech. Sci. 44 (2002) 825–841.
[15] W. Jiang, T.L. Wang, W.K. Jones, The forced vibration of helical spring, Int. J. Mech. Sci. 34 (1992) 549–563.
[16] J.W. Phillips, G.A. Costello, Large deflections of impacted helical springs, J. Acoust. Soc. Am. 51 (1971) 967–972.
[17] S.K. Sinha, G.A. Costello, The numerical solution of the dynamic response of helical springs, Int. J. Numer. Methods Eng. 12 (1978) 949–961.
[18] S. Ayadi, E. Hadj-Taieb, G. Pluvinage, The numerical solution of strain waves propagation in elastic helical springs, Mater. Technol. (2007) 47–52.
[19] S. Ayadi, E. Hadj-Taïeb, Influence des caractéristiques mécaniques sur la propagation des ondes de déformations linéaires dans les ressorts hélicoïdaux, Méc. Ind. 7 (2006) 551–563.
[20] S. Ayadi, E. Hadj-Taïeb, Simulation numérique du comportement dynamique linéaire des ressorts hélicoïdaux, Trans. Can. Soc. Mech. Eng. 30 (2) (2006) 191–208.
[21] S. Ayadi, A. Hamza, E. Hadj-Taïeb, Comportement dynamique des ressorts hélicoïdaux composites, in: Third International Congress Design and Modelling of Mechanical Systems CMSM'2009, Hammamet, Tunisia, 16-18 March 2009.
[22] P.D. Lax, B. Wendroff, Difference schemes for hyperbolic equations with high order of accuracy, Commun. Pure Appl. Math. 17 (1966) 381–398.
[23] A. Lerat, R. Peyret, Sur le choix des schémas aux différences du second ordre fournissant des profils de choc sans oscillations, C. R. Acad. Sci. Paris 277 (1966) 363–366.
[24] S. Ayadi, E. Hadj-Taieb, Finite element solution of dynamic response of helical springs, Int. J. Simul. Model. 7 (1) (2008) 17–28.
[25] C.E. Fröberg, Introduction to Numerical Analysis, Addison-Wesley Publishing Company, USA, 1979.
[26] V. Yildirim, Numerical buckling analysis of cylindrical helical coil springs in dynamic manner, Int. J. Eng. Appl. Sci. 1 (1) (2009) 20–32.